university of groningen

University Medical Center Groningen

University of Groningen

Equilibrium segregation at coherent (100) interfaces in ternary fcc systems analyzed using the cluster variation method

Kooi, Bart J.

Published in:
Acta Materialia

DOI:
10.1016/s1359-6454(03)00317-3

IMPORTANT NOTE: You are advised to consult the publisher's version (publisher's PDF) if you wish to cite from it. Please check the document version below.

Document Version
Publisher's PDF, also known as Version of record

Publication date:
2003

Link to publication in University of Groningen/UMCG research database

Citation for published version (APA):
Kooi, B. J. (2003). Equilibrium segregation at coherent (100) interfaces in ternary fcc systems analyzed using the cluster variation method. *Acta Materialia*, *51*(15), 4653-4665. https://doi.org/10.1016/s1359-6454(03)00317-3

Copyright
Other than for strictly personal use, it is not permitted to download or to forward/distribute the text or part of it without the consent of the author(s) and/or copyright holder(s), unless the work is under an open content license (like Creative Commons).

The publication may also be distributed here under the terms of Article 25fa of the Dutch Copyright Act, indicated by the “Taverne” license. More information can be found on the University of Groningen website: https://www.rug.nl/library/open-access/self-archiving-pure/taverne-amendment.

Take-down policy
If you believe that this document breaches copyright please contact us providing details, and we will remove access to the work immediately and investigate your claim.

Downloaded from the University of Groningen/UMCG research database (Pure): http://www.rug.nl/research/portal. For technical reasons the number of authors shown on this cover page is limited to 10 maximum.

Available online at www.sciencedirect.com
SCIENCE DIRECT®
Pergamon
Acta Materialia 51 (2003) 4653–4665
Acta MATERIALIA
www.actamat-journals.com

Equilibrium segregation at coherent (1 0 0) interfaces in ternary fcc systems analyzed using the cluster variation method

Bart J. Kooi *

Department of Applied Physics, Materials Science Centre, University of Groningen, Nijenborgh 4, 9747 AG Groningen, The Netherlands

Received 1 April 2003; received in revised form 28 May 2003; accepted 3 June 2003

Abstract

In order to study equilibrium segregation, composition profiles around coherent (1 0 0) interfaces in ternary fcc systems were calculated using the cluster variation method within the tetrahedron approximation. A comparison with a previous regular-solution (RS) based model was made for interfaces between two disordered phases. This RS model overestimates the maximum atomic fraction of the segregant at the interface when its bulk value is >0.1. The oscillatory decay in segregant concentration from its maximum at the interface to its bulk value is much less damped in the case of the RS model. Analysis of the damping behavior leads to a very good agreement with results from free energy expansion approximations. Finally, the CVM calculations were extended to interfaces between ordered ternary fcc phases or anti-phase boundaries. Results for the interface between the $L1_2$-$Cu_3Au(Ag)$ phase and a disordered Ag-rich phase in equilibrium at 583 K, and for a non-conservative APB in the same alloy, point to a strong suppression of order near the interfaces.
© 2003 Acta Materialia Inc. Published by Elsevier Ltd. All rights reserved.

Keywords: Interface segregation; Cluster variation method; Ordering; Interface antiphase; Ternary systems

1. Introduction

Interfacial segregation has received considerable theoretical and experimental attention in the past decades due to its potentially significant influence on materials properties [1]. Compared to segregation at surfaces and grain boundaries, segregation at heterophase interfaces has received only scant attention, both theoretically [1,2] and experimentally [1,3–6]. Recently, an experimental approach was developed to analyze Gibbsian segregation at heterophase interfaces using transmission electron microscopy, enabling the quantification of less than a monolayer coverage of the segregant at a planar hetero-interface [5,6]. The approach uses simple composition profiles as the input for fitting the experimental data. Usually it is assumed that the segregant is only enriched in a single monolayer at one side of the hetero-interface. One of the motivations for the present work

* Tel.: +31-50-3634896; fax: +31-50-3634881.
E-mail address: b.j.kooi@phys.rug.nl (B.J. Kooi).

1359-6454/03/$30.00 © 2003 Acta Materialia Inc. Published by Elsevier Ltd. All rights reserved.
doi:10.1016/S1359-6454(03)00317-3

is that the experimental approach would be improved if reliable theory-based composition profiles were available.

In the present work, equilibrium segregation at heterophase interfaces is modeled using the tetrahedron approximation in the cluster variation method (CVM) [7]. Based on ternary coherent fcc phase diagrams that can be computed using this method [8,9], coherent (1 0 0) interfaces are analyzed. The method used is to a large extent identical to that presented by Kikuchi and Cahn [7]. Their work was based on binary coherent fcc phase diagrams, explicitly including long-range order (LRO), and they analyzed anti-phase boundaries and interphase boundaries (i.e. between regions with LRO and SRO). One of their main objectives was to model the disordered wetting layer at APB's as a function of temperature below the critical one. This did not incorporate interfacial segregation because it was based on binary systems. The present work concentrates predominantly on segregation in ternary systems and LRO is not considered in the main part of this paper (disorder–disorder interfaces), although at the end an extension to order/disorder and APB's in $L1_2$ ordered ternary systems is made.

The accuracy of the method used by Kikuchi and Cahn [7] to obtain the concentration profiles was debated by Finel et al. [10,11]. The criticism holds in particular for the calculations performed near critical points such as the congruent point of Cu_3Au. In the present work, calculations for such critical points are avoided and the composition profiles obtained are accurate for the conclusions that are drawn.

The main objective of the present paper is to make a comparison between the CVM and the regular solution (RS) model of Dreggia and Wynblatt which also models the equilibrium segregation at coherent interfaces in ternary fcc systems [2]. It is generally recognized that the CVM gives better results than the RS models and the (Gorsky-) Bragg–Williams models in general, because it accounts for SRO [12]. Moreover, the present model does not require concentration profiles that are symmetrical with respect to the interface plane. The symmetrical case holds when the pair-wise interaction energies $w_{13} = w_{23}$, where the subscripts 1 and 2 are the solvent components rich on either side of the interface and subscript 3 is the solute component that may undergo segregation. Extension of the RS model [2] for $w_{13} \neq w_{23}$ is readily possible, but appears not trivial in practice due to, for instance, problems with convergence using the Newton–Raphson procedure, and therefore was probably not treated by Dreggia and Wynblatt.

Inputs for the modeling are the temperature and the three pair-wise interaction energies w_{12}, w_{13}, w_{23} ($w_{ij} = v_{ij} - (v_{ii} + v_{jj})/2$ with v_{ij} the nearest neighbor bond energy between atoms i and j). Outputs of the model are the concentration profiles ($x_n(i)$) with derived quantities such as interfacial excess concentration (Γ) or interfacial enrichment factor and interfacial energy (σ). An interesting finding is that the transition from the maximum concentration of the segregant at the interface to its bulk value under certain conditions obeys simple quantitative rules. If the interaction energy (w) between segregant and solute is less than zero, the transition from the maximum interfacial concentration to that in the bulk occurs by damped oscillations. For $w > 0$, the decay in concentration is monotonic. After about three planes away from the interface, the damping factor becomes constant in the case of the CVM, but it is not constant in case of the RS model. The damping factor is proportional to the reciprocal of the concentration of the segregant in the bulk for concentrations typically less than 5 at.%. Also a comparison is made between the present results and some predictions based on gradient thermodynamics [13] and free energy expansion approximations [14].

2. Theory

To a large extent, the calculation scheme used here is the same as that presented by Kikuchi and Cahn [7]. The complication here is that three instead of two atomic species are considered, but this in principle only changes the summation indices in the formulae. As a simple summary, we describe here the formulae used for the disorder–disorder interfaces, but they are easily extended to order–disorder, order–order interfaces and to anti-phase boundaries.

In the present calculations, when positioning the basic cluster in the multi-layer around the coherent fcc {1 0 0} interface, sites I and II in the tetrahedron are in plane n, sites III and IV are in plane $n+1$, with both planes parallel to the interface. In a ternary system, each site (I–IV) has a probability of being occupied by an atom species 1, 2 or 3. The probability that the configuration i, j, k, l (where i, j, k and l on sites I–IV, respectively, can each be independently 1, 2 or 3) appears on the cluster, with sites I and II in plane n, is denoted as z_n (i, j, k, l). In the absence of LRO, the probabilities of the pair (y within the plane and v across planes) and single site (x) variables are related to this basic variable through:

$$y_n(i,j) = \sum_{k,l} z_n(i,j,k,l)$$

$$v_n(i,k) = (v_n(i,l) = v_n(j,k) = v_n(j,l) =)\sum_{j,l} z_n(i,j,k,l)$$

$$x_n(i) = (x_n(j) =)\sum_{j,k,l} z_n(i,j,k,l) \tag{1}$$

Throughout the text these single-site occupation probabilities $x_n(i)$ will, for brevity, be referred to as concentrations and are thus defined per plane n. The whole concentration profile around the interface of a certain species i will be indicated by $x(i)$ and the constant values of the concentrations that hold far away from the interface, i.e. in the bulk, will be indicated by $x_b(i)$.

Since z_n overlaps with z_{n-1} and z_{n+1}, we have the continuity constraint:

$$y_n(i,j) = \sum_{k,l} z_n(i,j,k,l) = \sum_{k,l} z_{n-1}(k,l,i,j) \tag{2}$$

Of course the sum of all probabilities z_n (i, j, k, l) = 1:

$$\sum_{i,j,k,l} z_n(i,j,k,l) = 1 \tag{3}$$

In the case where only pair-wise nearest neighbor bonding is accounted for, the total energy E of a system of n planes each containing N sites is:

$$E = N\sum_{n}\sum_{i=1}^{3}\sum_{j=1}^{3}\sum_{k=1}^{3}\sum_{l=1}^{3} z_n(i,j,k,l)[w_{ij} + w_{ik} + w_{il} + w_{jk} + w_{jl} + w_{kl}] \tag{4}$$

with $w_{ij} = w_{ji}$, where $w_{ij} = v_{ij} - (v_{ii} + v_{jj})/2$ and v_{ij} is the nearest neighbor bond energy between atoms i and j. In ternary systems, this gives only three independent variables; w_{12}, w_{13}, w_{23}. The entropy, S, in case of the tetrahedron approximation is well known (see e.g. Refs. [7–9]) and is not repeated here. The grand potential, GP, is then defined as

$$GP = E - TS - (N/4)\sum_{n}\sum_{i=1}^{3}\sum_{j=1}^{3}\sum_{k=1}^{3}\sum_{l=1}^{3} z_n(i,j,k,l)[\mu_i + \mu_j + \mu_k + \mu_l] \tag{5}$$

with T, the temperature, and where, without loss of generality, the chemical potentials are related through $\mu_1 + \mu_2 + \mu_3 = 0$. The standard procedure is to fix one of the μ's and then varying the other two to find equilibrium values.

Finding the minimum in GP leads to the following set of 81n equations:

$$z_n(i,j,k,l) = z_n^0(i,j,k,l)\ \exp\left[\frac{\beta}{2}\lambda_n + \alpha_n(i,j) - \alpha_{n+1}(k,l)\right] \tag{6a}$$

with

$$z_n^0(i,j,k,l) = \exp\left[-\frac{\beta}{2}(w_{ij} + w_{ik} + w_{il} + w_{jk} + w_{jl} + w_{kl}) + \frac{\beta}{8}(\mu_i + \mu_j + \mu_k + \mu_l)\right][y_n(i,j)v_n(i,k)v_n(i,l)v_n(j,k)v_n(j,l)y_{n+1}(k,l)]^{1/2}[x_n(i)x_n(j)x_{n+1}(k)x_{n+1}(l)]^{-5/8} \tag{6b}$$

where $\beta = (kT)^{-1}$ with k, Boltzmann's constant, and λ and α are the Lagrange multipliers that take care of the constraints (3) and (2), respectively.

The calculation procedure is as follows. Certain values for the three ratio's w_{ij}/kT are considered (e.g. derived from theory or experiment). Since we are interested in the segregation of atom species 3 at the interface between an atomic species 1 rich phase (phase 1) on one side and an atom species 2 rich phase (phase 2) on the other side of the interface, w_{12} should be highly positive and w_{13} and w_{23}

positive to a lesser degree or even negative. Then the chemical potential of the segregant μ_3 is fixed and μ_2 is varied (with $\mu_1 = -(\mu_2 + \mu_3)$) until the GP's of both phases 1 and 2, showing phase separation, become equal. During this procedure the minimum in GP for each set of μ_i's is found by applying the natural iteration (NI) method [8,15] starting from initial guesses for $x(i)$ (and $y(i,j) = x(i)x(j)$). Then all variables are known for the bulk phases 1 and 2. Using the bulk $x(i)$ and $y(i,j)$ variables, the first estimation is made for the concentration profile within 20–40 planes on either side of the interface. At the interface, a step in the $x(i)$ and $y(i,j)$ occurs and $v(i,j) = y(i,j)$ except across the interface where $v(i,j)$ is initially estimated from $x_{phase1}(i)\ x_{phase2}(j)$. Then the first step in using the NI method for solving the concentration profiles is performed. In each step, the $81n$ z_n^0 are calculated using Eq. (6b), followed by the iterative solution of the $9n-\alpha$ (see Appendix A on this minor iteration) after which the $n-\lambda$ can be easily determined. Each step supplies output values for $x(i)$, $y(i,j)$ and $v(i,j)$ that are used as new inputs in Eq. (6b) for the next major step of the iteration. The NI method is continued until the changes in the output variables become sufficiently small; 300–600 iterations were typically sufficient for the disorder/disorder interfaces. At the interfaces involving an ordered phase, convergence occurred more slowly and in some cases up to 5000 iterations were required.

3. Results and discussion

3.1. Disorder–disorder interfaces

The purpose of the present section is to show the general trends in concentration profiles for hetero-interfaces in ternary systems and for this reason a connection to a specific ternary system is avoided. A typical composition profile for $w_{12}/kT = 1.5$, $w_{13}/kT = 0.15$ and $w_{23}/kT = -0.45$ with $\mu_3/kT = -4.5$ is shown in Fig. 1. These values for w_{ij}/kT are realistic. For example, in Ref. [9] for the Cu–Au–Ag ternary phase diagram, $w_{12}/kT = -1.326$, $w_{13}/kT = 0.472$ and $w_{23}/kT = -1$ at $T = 500$ K were used. The chemical potential μ_3 determines

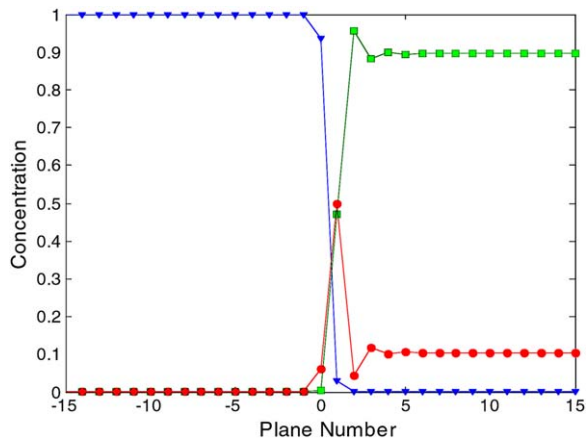

Fig. 1. The composition profile around a coherent (1 0 0) interface in a ternary fcc system for $w_{12}/kT = 1.5$, $w_{13}/kT = 0.15$ and $w_{23}/kT = -0.45$ with $\mu_3/kT = -4.5$.

the concentrations $x_b(3)$ in the bulk phases 1 and 2 on either side of the interface. The chemical potentials μ_1 and μ_2 are such that equilibrium pertains between the phases 1 and 2. It is clear that atom species 3 segregates relatively strongly with a maximum concentration $x(3)$ of just over 0.5 compared to $x_b(3)$ of 10^{-4} in phase 1 and 0.1 in phase 2. Of course this maximum concentration occurs at the interface in the first monolayer of phase 2 (plane number 1). The decay of the concentration $x(3)$ is monotonic and large in phase 1 where w_{13} is positive, but is more gradual and exhibits an oscillatory behavior in phase 2 where w_{23} is negative.

As a comparison of the present CVM model with the one of the RS model proposed in a previous study [2], Fig. 2 shows some results for the case $w_{13} = w_{23}$ ($w_{12}/kT = 1.5$, $w_{13}/kT = -0.45$, $w_{23}/kT = -0.45$). These parameters were also used for Figs. 3–10. Fig. 2a shows the CVM results and Fig. 2b the corresponding results for the RS model. For relative small values of $x_b(3)$ the results of both models are in reasonable agreement. However, upon increasing $x_b(3)$, two differences become increasingly pronounced: (i) the maximum concentration of $x(3)$, at the interface is greater for the RS than for the CVM model, and (ii) the oscillations characteristic for the decay in $x(3)$ from its maximum to bulk value are less damped in case of the RS model.

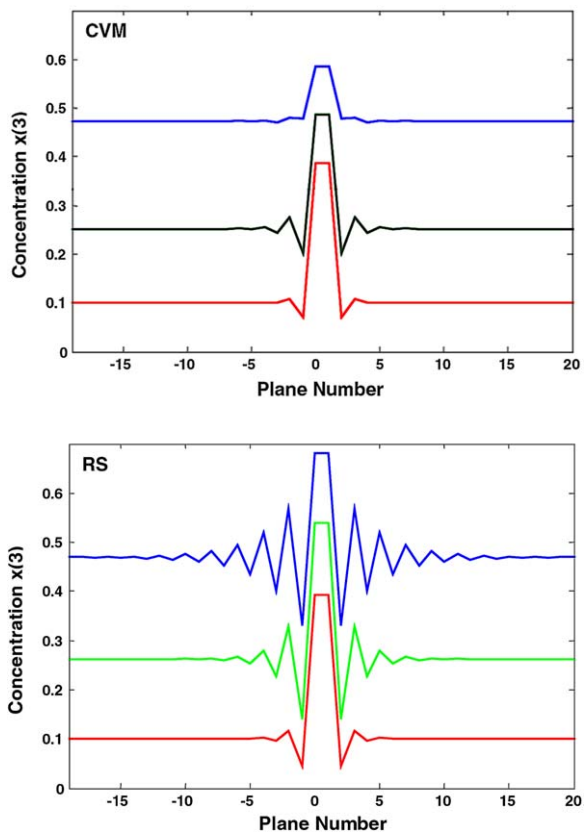

Fig. 2. The concentration profiles for $w_{12}/kT = 1.5$, $w_{13}/kT = -0.45$ and $w_{23}/kT = -0.45$ for three different values of μ_3/kT (i.e. three different low bulk $x_b(3)$ concentrations), for (a) the CVM and (b) the RS model.

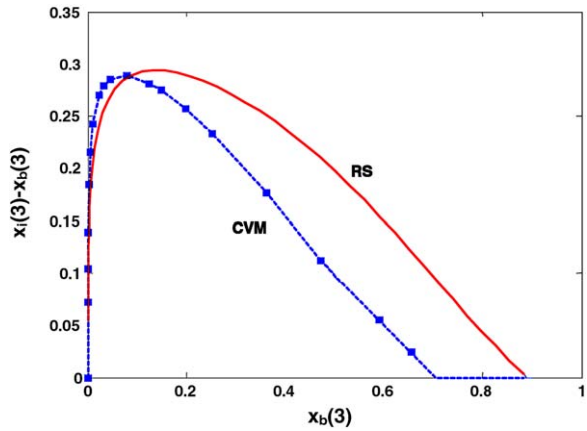

Fig. 3. The difference between the maximum concentration at the interface $x_i(3)$ and the bulk $x_b(3)$ concentration as a function of $x_b(3)$ according to the CVM and the RS model ($w_{12}/kT = 1.5$, $w_{13}/kT = -0.45$ and $w_{23}/kT = -0.45$).

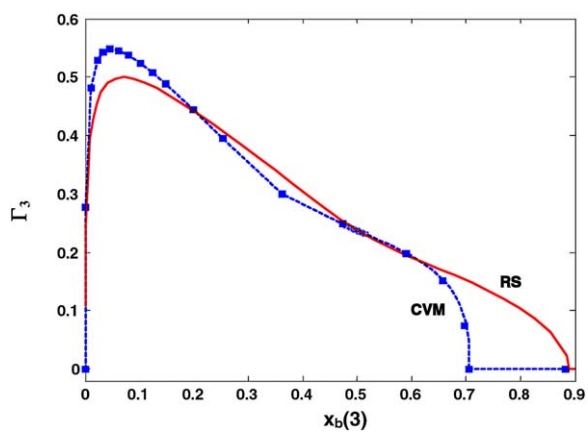

Fig. 4. The excess concentration τ_3 due to the interface as a function of the bulk $x_b(3)$ concentration according to the CVM and the RS model ($w_{12}/kT = 1.5$, $w_{13}/kT = -0.45$ and $w_{23}/kT = -0.45$).

Fig. 3 shows the difference between the maximum concentration at the interface and that of the bulk as a function of $x_b(3)$ for the total range 0–1 for both the CVM and the RS model. For small $x_b(3)$ values, the CVM model predicts a slightly greater maximum concentration at the interface than the RS model, but then the RS model overestimates the maximum concentration of the segregant. To a large extent this can be explained by the value for $x_b(3)$ where the interface between phase 1 and 2 disappears because phase separation vanishes (i.e. the concentrations in phase 1 and 2 become identical). This critical value is higher in the RS than the CVM model. This is logical because both models use the same w_{ij} values and thus will always lead at a certain temperature to a broader region of phase separation in the phase diagram based on the RS model. This broader region in the RS model is a direct consequence of neglecting SRO, which makes phase separation between phases rich in atom species 1 and 2 already more energetically favorable at smaller concentrations of $x(1)$ and $x(2)$.

The total excess in $x(3)$, Γ_3, based on a summation over 20 planes on either side of the interface is shown in Fig. 4 as a function of $x_b(3)$ for

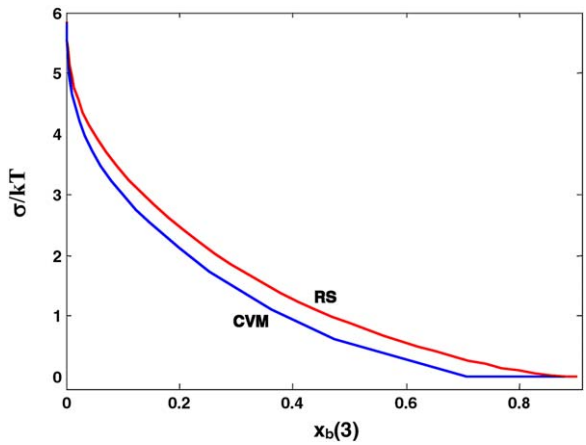

Fig. 5. The interfacial energy σ/kT as a function of the bulk $x_b(3)$ concentration for the CVM and the RS model ($w_{12}/kT = 1.5$, $w_{13}/kT = -0.45$ and $w_{23}/kT = -0.45$).

the total range 0–1 for both the CVM and the RS model. Compared to Fig. 3, the difference between the results of the CVM and the RS model in Fig. 4 is relatively small for $x_b(3) > 0.2$. The difference in maximum concentration at the interface between the CVM and the RS model is compensated by the oscillatory nature of the decaying concentrations in the planes adjacent to the interface, where the amplitude of the oscillations is larger for the case of the RS model.

The interfacial energy, σ, defined as the excess free energy or excess of the grand potential, is shown as a function of $x_b(3)$ for the total range 0–1 in Fig. 5 for the CVM and the RS models. Using the same input parameters as above, the composition profiles predicted using the CVM model correspond to a smaller interfacial energy than the profiles predicted using the RS model. Again the absence of SRO forces the RS model to these erroneously high interfacial-energy values.

A negative value for w_{13} or w_{23} does not necessarily mean that the oscillations in the concentration profiles are present under all conditions. When the concentration $x_b(3)$ is approaching its maximum value in the miscibility gap the oscillations disappear, leading to a relative slow monotonic decay (see Fig. 6). This holds for both the CVM and the RS model, but the enrichment in $x(3)$ tends to extend over a larger number of planes in the case of the CVM model.

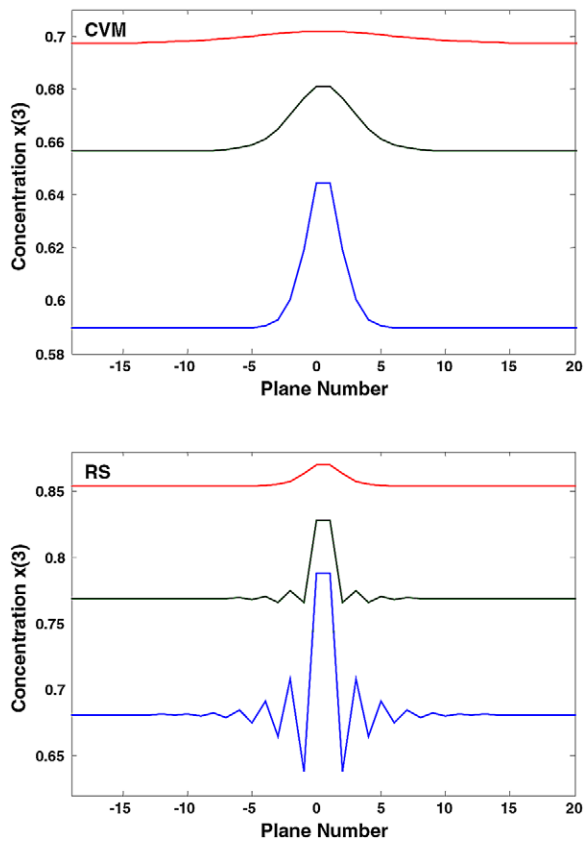

Fig. 6. Concentration profiles for $w_{12}/kT = 1.5$, $w_{13}/kT = -0.45$ and $w_{23}/kT = -0.45$ for three different values of μ_3/kT (i.e. three different high bulk $x_b(3)$ concentrations), for (a) the CVM and (b) the RS model.

The damping of the oscillations can be quantified by dividing the difference in concentration between planes $n-1$ and n by the difference in concentration between planes n and $n+1$ further from the interface. Results for this decay ratio or damping factor, $\tau_n = (x_{n-1}-x_n)/(x_n-x_{n+1})$, for both the CVM and the RS model are shown in Fig. 7a,b where $x_b(3)$ is close to 0.14 and 0.07, respectively (cf. Fig. 2). Fig. 7 clearly shows that a constant τ (often up to five digits) holds from a few planes away from the interface in case of the CVM. In case of the RS model, the damping factor is in general not constant. The negative value of τ indicates an oscillatory nature of the decaying concentration and is positive for a monotonic decay. Comparison of τ for different temperatures but the same

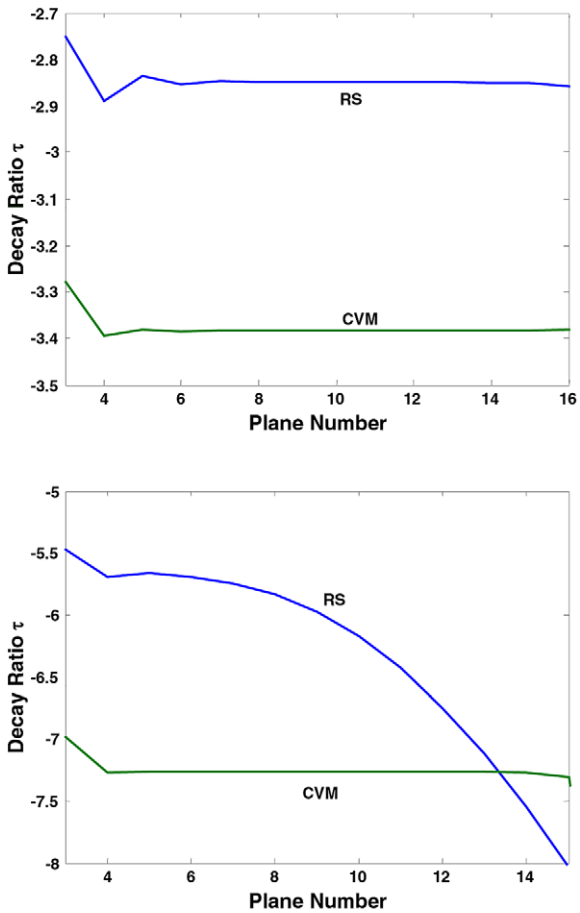

Fig. 7. The decay ratio or damping factor $\tau_n = (x_{n-1}-x_n)/(x_n-x_{n+1})$ as a function of distance away from the interface for the CVM and the RS model for $x_b(3)$ close to (a) 0.14 and (b) 0.07 (cf. Fig. 2).

$x_b(3)$ concentration shows that the higher the temperature (approaching the critical temperature in the miscibility gap) the larger the absolute value of τ. Furthermore, the smaller $x_b(3)$ the larger the absolute value of τ for the same temperature. Fig. 8 shows the relationship between τ and $x_b(3)$ on a log–log scale. The data points on the dashed line are based on the results of the CVM and the straight line is added to indicate a slope of -1. It is clear that at sufficient low concentrations of $x_b(3)$ (here below 5 at.%), the relation between τ and $x_b(3)$ is:

$$\tau = -\frac{C}{x_b(3)} \tag{7}$$

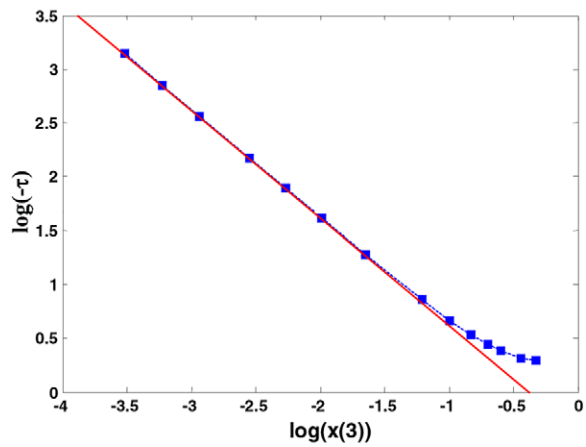

Fig. 8. The decay ratio or damping factor τ as a function of $x_b(3)$ concentration for the CVM model showing that τ is proportional to the reciprocal of $x_b(3)$ for $x_b(3) < 0.1$.

with C a positive constant. To the author's knowledge, no previous literature exists on the analysis of the decaying oscillatory concentrations for ternary alloys. However, in the mean-field analysis of surface segregation in binary systems, the damping factor plays an important role in obtaining a mathematically stable method, using the so-called area-preserving map for calculating concentration depth profiles [16]. In principle, the method holds for planes at significant depths and for small concentration differences with the bulk concentration. Applying the method to the Bragg–Williams approximation and to two different free-energy expansion approximations yields the following damping factor τ if the {1 0 0} plane of an fcc binary system is parallel to the surface [14]:

$$\frac{1}{\tau} = -\frac{r}{2} \pm \sqrt{\frac{r^2}{4}-1}, \tag{8a}$$

$$r = \frac{2V + (4c(1-c))^{-1} + f(V)\{10c(1-c)-1\}}{2V + f(V)\{4c(1-c)-1\}}, \tag{8b}$$

BW approximation:

$$f(V) = 0, \tag{8c}$$

$$\Delta\bar{F}_2^{\mathrm{SRO}}: f(V) = V^2, \tag{8d}$$

FCEM approximation:

$$f(V) = \exp(-2V) + 2V - 1, \tag{8e}$$

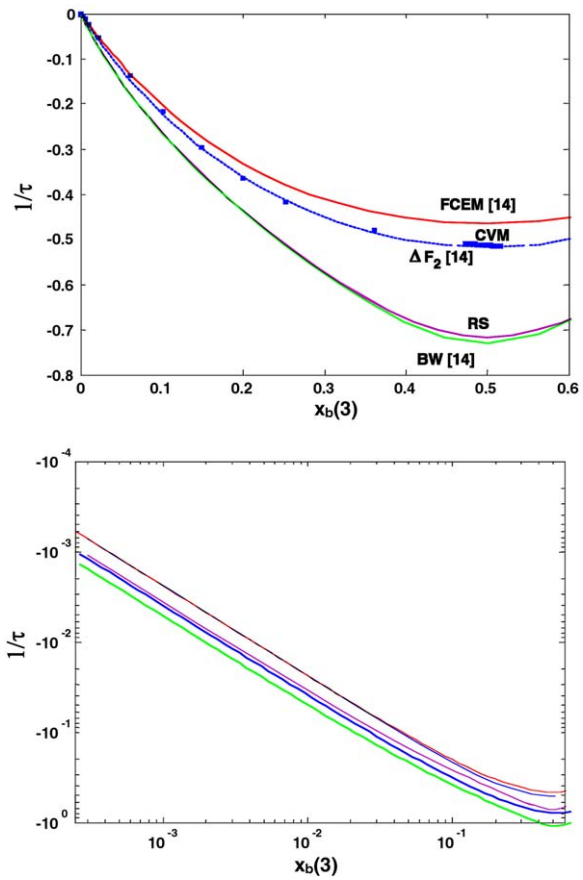

Fig. 9. The decay ratio or damping factor τ as a function of $x_b(3)$ concentration according to several models (see text) in a plot with normal (linear) axes (a) and with logarithmic axes (b).

$$V = -\frac{w_{12}}{kT} \tag{8f}$$

The plus sign in Eq. (8a) holds for alloys that undergo ordering ($V > 0$) with an oscillatory depth profile and the minus sign for phase-separating alloys ($V < 0$) with a monotonic decaying concentration profile. $\Delta\bar{F}_2^{\mathrm{SRO}}$ is the first order correction term in the inverse temperature cumulant expansion of the free energy, starting from the BW approximation to account for SRO. It in principle only holds for $V > 0$ and for $V < 0$ it should be replaced by $2V^2$ [14]. It's accuracy increases as the value of V approaches zero. The FCEM approximation introduces an SRO correction to the free-energy description of the BW approximation that

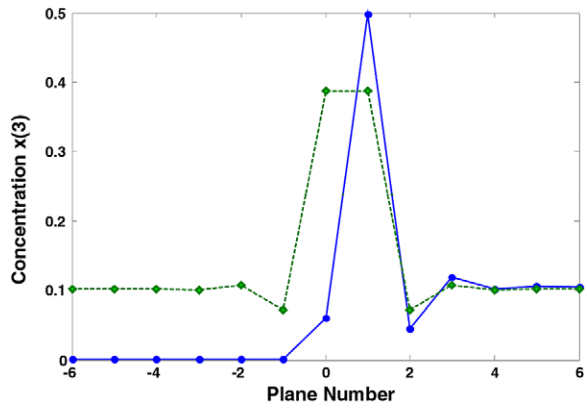

Fig. 10. Concentration profile around a coherent (1 0 0) interface in a ternary fcc system for $w_{12}/kT = 1.5$, $w_{13}/kT = 0.15$ and $w_{23}/kT = -0.45$ (solid line) and $w_{12}/kT = 1.5$, $w_{13}/kT = -0.45$ and $w_{23}/kT = -0.45$ (dashed line), showing that there is a clear mutual interaction across the interface with an extend of about five monolayers.

becomes exact in the dilute limit [14]. A comparison between the present results (i.e. with the CVM and the RS model) and the results of Eq. (8) ($V = 0.45$) as a function of $x_b(3) = c$ concentration is given in Fig. 9. The same results are shown in the log–log plot in Fig. 9b for comparison with the linear plot in Fig. 9a. The results provide the following important insights:

1. The results according to the RS model and the BW approximation are nearly identical, even more so than expected because the results of Eq. (8), as applied to binary alloys, are exactly symmetric with respect to the concentration $c = 0.5$. This is of course not the case for the CVM and the RS model for ternary systems. In the latter case even the damping factor changes sign when approaching the maximum $x_b(3)$ in the miscibility gap, as in Fig. 6, where the oscillations change gradually into a monotonic decay. Furthermore, the damping factor is not constant and thus, not strictly defined in the RS model. This may also result in slight deviations from the BW prediction.
2. The results of the CVM and the FCEM approximation are the same for dilute alloys in the present case for $x_b(3) = c < 0.03$. This is in accordance with the SRO correction of the

FCEM approximation becoming more accurate the more diluted the system becomes.

3. The results according to the CVM and the $\Delta\bar{F}_2^{SRO}$ expansion are very similar for $x_b(3) = c > 0.1$). So, in the range $0.03 < c < 0.1$, a transition occurs where the CVM result begins to deviate significantly from the FCEM and become increasingly similar to the $\Delta\bar{F}_2^{SRO}$.
4. Both the CVM, $\Delta\bar{F}_2^{SRO}$ and FCEM approximations show that the damping factor in case of the RS model or the BW approximation is too small (i.e. oscillations remain too large).
5. The damping factor of the FCEM approximation becomes too large (using the CVM as a reference) for the non-diluted case, where its accuracy diminishes. The damping factor of the $\Delta\bar{F}_2^{SRO}$ expansion becomes too small for the diluted case.
6. All the curves in Fig. 9b show that the damping factor τ is inversely proportional to $x_b(3) = c$ (Eq. (7)) for diluted alloys. The CVM exhibits this behavior up to the highest concentration, followed by FCEM, then $\Delta\bar{F}_2^{SRO}$ and finally the RS/BW approximation.

In summary, it is demonstrated that in the phase-separating case presented here, some results of binary alloys can be used to predict behavior of ternary systems. However, this is not surprising, since the above CVM and RS calculations do not hold for a proper ternary alloy, but for a pseudo-binary one. The role of atomic species 1 and 2 are interchanged on both sides of the interface, but the segregation of atomic species 3 is symmetric around the interface as for a grain boundary in a binary system.

For a proper ternary system, Fig. 10 shows that there is mutual interaction across the interface. The only difference between the initial parameters used to calculate the two concentration profiles is that the dashed line holds for the pseudo-binary interface with $w_{13}/kT = w_{23}/kT = -0.45$, whereas the solid line holds for a proper ternary system with $w_{13}/kT = 0.1$, $w_{23}/kT = -0.45$. On the right side of the interface similar results can be expected. Nevertheless, planes 1–5 show clear differences that are invoked by the different conditions on the left side of the interface.

A general model-independent prediction of gradient thermodynamics is that the tail of the surface/interface composition profile in a binary alloy decays exponentially to the bulk composition [13]. In the present context this means that such a composition profile is characterized by a monotonic decay with a *constant positive* value for the decay ratio τ. However, the present analysis shows that this prediction of gradient thermodynamics should be interpreted more generally where an exponential decay also includes the possibility of an oscillatory decay with a *constant negative* value for the decay ratio τ.

3.2. Order–disorder interfaces

Calculation of the previous type of ternary composition profiles can easily be extended within the same CVM framework to interfaces where ordered fcc alloys such as $L1_2$ or cubic $L1_0$ are present on one or both sides of the interface. As an example, the result for the coherent (1 0 0) interface in the Cu–Ag–Au system was calculated between ordered Cu_3Au (with small amount of Ag in solution) and disordered AgAu (with small amount of Cu in solution). The pair interaction energies were taken from the CVM calculations of the Cu–Ag–Au phase diagram [9]: $w_{Cu-Ag}/k = 236$ K, $w_{Cu-Au}/k = -663$ K and $w_{Ag-Au}/k = -500$ K. The chemical potential μ_{Au}/kT was set to -5. Equilibrium between the $L1_2$ Cu-rich phase and the disordered Ag-rich phase was attained for μ_{Ag} close to 3 while keeping $\mu_{Cu} + \mu_{Ag} + \mu_{Au} = 0$. Fig. 11 shows the composition profiles around the interface at a temperature of 583 K. On the ordered side of the interface, each second (1 0 0) plane contains two different types of sites (planes -20 up to -1). Due to the $L1_2$ nature of the ordering, one of these sites is similar (becoming identical far from the interface) to the two sites in the adjacent (1 0 0) planes. Note that Ag prefers to occupy the Cu-rich sites and not the Au-rich site in Cu_3Au.

In the calculations one can choose to have immediately at the interface a (1 0 0) plane of $L1_2$ with either the two identical or the two different types of sites. Apart from a shift with one (1 0 0) plane, the resulting composition profiles are identical (as verified). However, the calculation of the

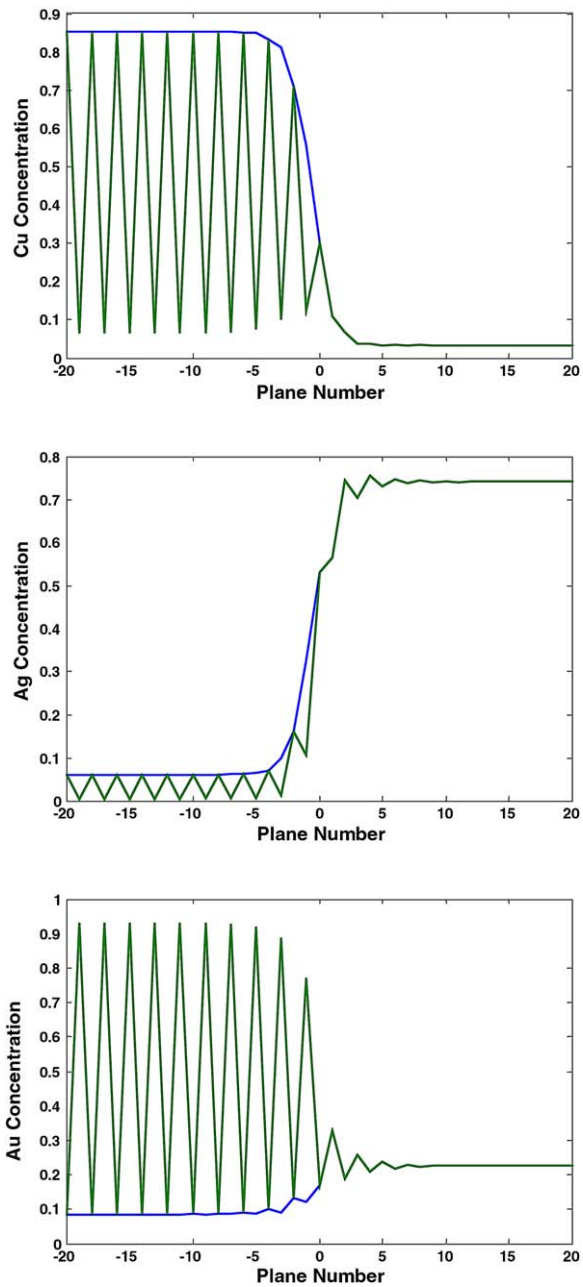

Fig. 11. Concentration profiles around a coherent (1 0 0) interface in the Cu–Ag–Au system at 583 K. On the left side of the interface $L1_2$ ordered Cu_3Au (with small amount of Ag) and on the right side disordered AgAu (with small amount of Cu) is present. The pair interaction energies were taken from the CVM calculations of the Cu–Ag–Au phase diagram [9]: w_{Cu-Ag}/k = 236 K, $w_{Cu-Au}/k = -663$ K and $w_{Ag-Au}/k = -500$ K.

interfacial excess concentrations, Γ_i, is now ambiguous because plane 0 in Fig. 11 can be assigned in either the $L1_2$ Cu-rich phase or the disordered Ag-rich phase. The lowest excess concentrations for all three atomic species occur when plane 0 is attributed to the Ag-rich phase. Cu is depleted at the interface ($\Gamma_{Cu} = -0.228$) with a strong depletion on the $L1_2$ side (-0.602) and excess at the Ag-rich side (+0.374). Ag is enriched at the interface ($\Gamma_{Ag} = +0.245$) with large excess at the $L1_2$ side (-0.649) and depletion on the Ag-rich side (+0.404). Finally Au shows a very small depletion ($\Gamma_{Au} = -0.017$) with depletion at the $L1_2$ side (-0.046) and excess at the Ag-rich side (+0.030). Qualitatively, the results for Cu and Ag are the same if plane 0 is attributed to the $L1_2$ phase. This is not the case for Au for it shows an excess ($\Gamma_{Au} = +0.213$) with excess on the $L1_2$ side (0.126) and excess on the Ag-rich side (0.087). From the unambiguous depletion of Cu and the excess of Ag, it is clear that at the interface there is a tendency to move away from the $L1_2$-ordered Cu_3Au(Ag) within the 2-phase region towards the disordered Ag-rich phase. In this sense, it can be concluded that due the presence of the interface, the disordered Ag-rich phase is slightly favored over the ordered Cu-rich phase. Moreover, it is also clear from Fig. 11 that the degree of order in $L1_2$ decreases and vanishes on approaching the interface. This result agrees with the width of the Al_3Li–Li interface calculated in Ref. [17], where it was shown that this width is a linear function of the temperature over a wide range, without an indication that it diverges to infinity at the transition temperature.

3.3. Anti-phase boundaries

Using the same CVM calculations, the composition profiles around a non-conservative APB within a ternary $L1_2$ phase can also be calculated. An example is given in Fig. 12 for an APB within the $L1_2$ Cu_3Au(Ag) phase that was used in the previous section. From Fig. 12 it is clear that approaching the APB, the degree of order decreases and the concentrations for the two (1 0 0) planes at the core of the APB approach the average concentrations in bulk $L1_2$ as if ordering was

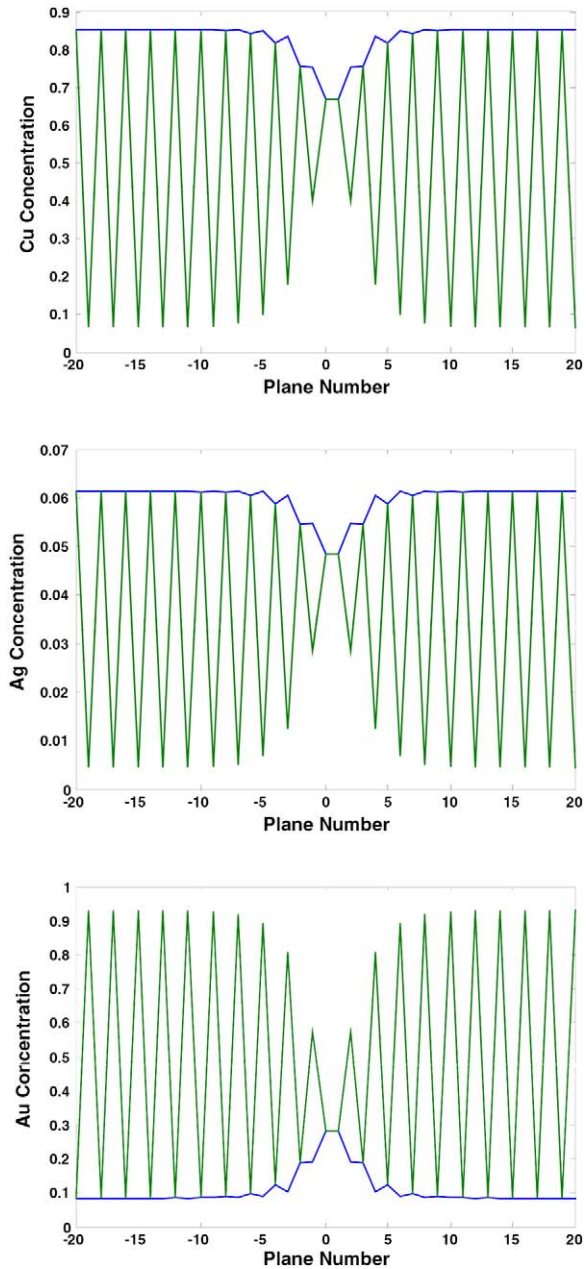

Fig. 12. Concentration profiles around an anti-phase boundary in $L1_2$ ordered Cu_3Au (with small amount of Ag) at 583 K. The pair interaction energies were taken from the CVM calculations of the Cu–Ag–Au phase diagram [9]: w_{Cu-Ag}/k = 236 K, $w_{Cu-Au}/k = -663$ K and $w_{Ag-Au}/k = -500$ K.

absent. The lower the temperature, the more the concentrations in these two (1 0 0) planes will deviate from the average concentration and approach that of the corresponding planes in the ordered phase far away from the APB. The higher the temperature, the more the concentrations in these two (1 0 0) planes approach the average concentration in bulk $L1_2$ phase. In this sense, the two (1 0 0) planes at the APB core are always in a state in-between the ordered bulk and the fully disordered one, and so still correspond to a small finite degree of ordering. Only very near to the critical temperature is true disordering (i.e. wetting of the APB) anticipated, where the width of the wetting layer is proportional to $\log(T_C - T)^{-1}$ [10,11].

Calculation of interfacial excess concentrations due to the presence of the APB is not ambiguous in contrast to the previous section. Around the APB, a depletion of Cu is present with a total of $\Gamma_{Cu} = -0.306$, a depletion of Ag with $\Gamma_{Ag} = -0.018$ and an excess of Au with $\Gamma_{Au} = +0.323$. Note that in contrast to these values in the two (1 0 0) layers at the core of the APB (planes 0 and 1) the Cu and Ag concentration are, (and in fact have to be) higher and the Au concentration is (and has to be) lower than the corresponding average concentrations in the bulk $L1_2$ phase. So, the excess/depletion is steered by the adjacent planes, in particular planes -1 and 2. For instance, in planes 0 and 1, independent of temperature (below T_C) there is always an excess of Cu, so, whether an overall depletion or an excess of Cu holds, is determined mainly by planes -1 and 2. Note that the $L1_2$ Cu_3Au(Ag) considered here is in equilibrium with the disordered Ag-rich phase as in the previous section.

Based on the known Cu–Ag–Au phase diagram as calculated using the CVM [9], the excess concentrations indicate that on either side of the APB the concentrations tend to move away from the equilibrium with the Ag-rich phase to within the $L1_2$ single-phase field. Of course a more complicated situation would have occurred if near/at the APB the concentrations would have entered the two-phase region, possibly making the APB in Cu_3Au unstable with respect to the Ag-rich phase. Then a disordered wetting layer could develop at

the APB that is of a different nature to that analyzed for the binary Cu–Au system [7,10,11]. However, although the present results are very limited and relatively far below T_C, they seem to indicate that such a wetting layer will not develop. Nevertheless, a thorough analysis of APB's in $L1_2$ Cu_3Au(Ag) in equilibrium with a Ag-rich phase near T_C remains an interesting issue, because may show a novel type of wetting behavior.

4. Conclusions

Equilibrium segregation at coherent (1 0 0) hetero-interfaces in ternary fcc systems was analyzed using the cluster-variation method within the tetrahedron approximation.

For disorder–disorder interfaces, clear differences were observed between the present CVM model and a regular-solution model of Dreggia and Wynblatt [2], particularly if the equilibrium concentration of the segregating element in the bulk phase is appreciable (>0.1). In this case, the RS model overestimates values for the maximum concentration of the segregant at the interface. Furthermore, the decay in segregant concentration from its maximum at the interface to its bulk value is much less damped in case of the RS model. If the segregating element shows an ordering tendency with the element rich in the bulk, the segregant concentration decay is oscillatory. The damping of these oscillations occurs by a constant factor in case of the CVM model. This damping factor, τ is proportional to the reciprocal of the equilibrium concentration of the segregating element in the bulk, $x_b(3)$, for $x_b(3) < 0.1$. Analytical predictions for τ of binary systems according to two different free-energy expansion approximations are in certain concentration intervals the same as τ according to the present CVM calculations for $w_{13} = w_{23}$; FCEM is the same for $0 < x_b(3) < 0.03$ and $\Delta\bar{F}_2^{\mathrm{SRO}}$ is the very similar for $0.1 < x_b(3) < 0.5$.

At order–disorder interfaces, a gradual decrease and vanishing of the order occurs at finite temperatures below T_C when approaching the interface. For the calculated interface between $L1_2$ Cu_3Au(Ag) and disordered Ag-rich phase at 583 K, a depletion of Cu and an excess of Ag is observed, i.e. a stabilization with respect to the disordered Ag-rich phase occurs. At a non-conservative APB in $L1_2$ Cu_3Au(Ag) at 583 K, a gradual decrease of order occurs and the two (1 0 0) planes at the APB have a concentration approaching the average of the $L1_2$ phase. Due to the APB, a depletion of Cu and an excess of Au is present, which makes the formation of a disordered Ag-rich wetting layer at the APB in Cu_3Au unlikely.

Appendix A

Eq. (6a) in Section 2 can be rewritten as:

$$z_n(i,j,k,l) = z_n^0(i,j,k,l)\,\frac{a_n(i,j)}{a_{n+1}(k,l)}\exp\left[\frac{\beta}{2}\lambda_n\right] \tag{A.1}$$

Combining the continuity constraint Eq. (2) with Eq. (A.1), it follows that:

$$y_n(i,j) = \exp\left[\frac{\beta}{2}\lambda_n\right]\sum_{k,l} z_n^0(i,j,k,l)\,\frac{a_n(i,j)}{a_{n+1}(k,l)} \tag{A.2a}$$

$$y_n(i,j) = \exp\left[\frac{\beta}{2}\lambda_{n-1}\right]\sum_{k,l} z_n^0(k,l,i,j)\,\frac{a_{n-1}(k,l)}{a_n(i,j)} \tag{A.2b}$$

Based on Eq. (A.2), the following two functions can be defined:

$$g_n(i,j) = y_n(i,j)/a_n(i,j) = \exp\left[\frac{\beta}{2}\lambda_n\right]\sum_{k,l} z_n^0(i,j,k,l)/a_{n+1}(k,l) \tag{A.3a}$$

$$h_n(i,j) = y_n(i,j)*a_n(i,j) = \exp\left[\frac{\beta}{2}\lambda_{n-1}\right]\sum_{k,l} z_n^0(k,l,i,j)*a_{n-1}(k,l) \tag{A.3b}$$

Combining Eq. (A.3a) and (A.3b) yields:

$$a_n(i,j) = \sqrt{\frac{h_n(i,j)}{g_n(i,j)}} \tag{A.4}$$

The iterative procedure to solve $a_n(i,j)$ is as follows. After $z_n^0(i,j,k,l)$ is calculated using Eq. (6b), $g_n(i,j)$ and $h_n(i,j)$ are determined using Eq. (A.3) incorporating the $a_n(k,l)$ values of the previous

major iteration step connected to the natural iteration scheme. From Eq. (A.4), the new values for a_n are determined and inserted again in Eq. (A.3). This use of Eqs. (A.3) and (A.4) is repeated until the a_n values converge to within of 10^{-14}. For this minor iteration procedure performed each major step of the NI method typically 20–30 iterations are used initially during the major iteration, but finally when $z_n(i,j,k,l)$ converges, the number of iterations decreases to about 10.

References

[1] Johnson WC, Blakeley JM. Interfacial segregation. Metals park (OH): American Society for Metals, 1977.
[2] Dreggia SA, Wynblatt P. Acta Metall. Mater. 1991;39:771.
[3] Hayes P, Grieveson P. Met. Sci. 1995;9:332.
[4] Shaskov DA, Muller DA, Seidman DN. Acta Mater. 1999;47:3953.
[5] Kooi BJ, Wouters O, De Hosson JTM. Acta Mater. 2002;50:223.
[6] Mogck S, Kooi BJ, De Hosson JTM. Phil. Mag. 2003;83:727.
[7] Kikuchi R, Cahn JW. Acta Metall. 1979;27:1337.
[8] Kikuchi R. Acta Metall. 1977;25:195.
[9] Kikuchi R, Sanchez JM, De Fontaine D, Yamauchi H. Acta Metall. 1980;28:651.
[10] Finel A, Mazauriac V, Ducastelle F. Phys. Rev. Lett. 1990;65:1016.
[11] Finel A. In: Yavari AR, editor. Proceedings of the workshop “Ordering and disordering in alloys”, Grenoble, July 1991. New York: Elsevier Applied Science; 1992.
[12] Ducastelle F. Order and phase stability in alloys. North-Holland: Amsterdam, 1991.
[13] Cahn JW. Interfacial segregation. In: Johnson WC, Blakeley JM, editors. Metals park (OH): American Society for Metals; 1977. p. 11.
[14] Polak M, Rubinovich L. Surf. Sci. Reports 2000;38:127.
[15] Kikuchi R. J. Chem. Phys. 1974;60:1071.
[16] Legrand B, Treglia G, Ducastelle F. Phys. Rev. B 1990;41:4422.
[17] Sluiter M, Kawazoe Y. Phys. Rev. B 1996;54:10381.